A PROJECTION-BASED MODEL ORDER REDUCTION SIMULATION TOOL FOR SPACECRAFT THERMAL ANALYSIS

Yi Wang*, Hongjun Song, Kapil Pant
CFD Research Corporation, Huntsville AL, USA (*Email: yxw@cfdrc.com)

Hume Peabody, Jentung Ku, Charles D. Butler
Thermal Engineering Branch, NASA Goddard Space Flight Center, Greenbelt, MD, USA

ABSTRACT

Accurate, efficient thermal analysis is a well recognized challenge for accurate spacecraft design and control. This paper presents a novel research effort aimed at the development of mathematically rigorous Model Order reduction (MOR) algorithms, as well as an integrated framework to automatically generate reduced thermal models of spacecrafts for computation by fast, efficient Differential-Algebraic Equation (DAE) solvers. Two testbed models consisting of constant sources, capacitances, and conductances with approximately 600 and 3000 nodes were used to evaluate a Trajectory Piecewise Linear Model Order Reduction (TPWLMOR) algorithm. The full-scale models were reduced to a low-dimensional model with 64 nodes. The overall MATLAB solution of the reduced model took about ~1 second compared to ~10 seconds and ~300 seconds for the full-scale solution. A comparison of reduced order model against the full-scale solution shows excellent agreement with the maximum absolute nodal temperature error spanning from -2.8°C to +2.9 °C (largely between -1 °C and +1 °C) and the average relative error < 0.5%. While some computational expense is incurred to generate the reduced model, its reusability enables significant savings in computational times and resources for transient simulation and analysis. The case studies firmly establish the feasibility of our MOR technique for spacecraft thermal analyses of NASA relevance.

INTRODUCTION

Trends in recent years have been towards larger thermal models and have therefore placed additional computational demands on the thermal engineer. Attempts to verify designs by modeling and analysis rather than testing further this burden. Current analysis tools heavily rely on high-fidelity simulations that are computationally prohibitive and require a significant level of expertise from spacecraft design engineers, leading to substantial cost overruns and delays in spacecraft development. Therefore, there is a clear and unmet need for a software tool that can automate the generation of mathematically rigorous, reduced thermal models (from large models) to enable order-of-magnitude enhancements in computational resources and analysis time leading to efficient spacecraft design.

To address these critical needs, CFD Research Corporation (CFDRC) is developing mathematically rigorous model order reduction (MOR) algorithms and simulation tools to automatically generate reduced thermal models amenable to fast computation by efficient Ordinary-Differential Equation/Differential-Algebraic Equation (ODE/DAE) solvers. The underlying principle of our MOR tool is to approximate a dynamic system response through projection onto a low-dimensional subspace constructed by a combination of characteristic orthonormal basis vectors of the system.

In this paper, we report on MOR algorithm development and model demonstration for selected testbed models consisting of constant sources, capacitances, and conductances with approximately 600 and 3000 nodes using a Trajectory Piecewise Linear Model Order Reduction (TPWLMOR) algorithm. The full-scale models were reduced to a low-dimensional model with 64 nodes by the TPWLMOR yielding orders-of-magnitude speed up in the analysis time. A comparison of the reduced order model against the full-scale model results showed excellent agreement with the average relative error of less than 0.5%. To the best of authors' knowledge, our work represents the first effort to apply mathematically rigorous, nonlinear MOR algorithms to spacecraft thermal analysis for automated generation of reduced thermal models and to develop a modular framework to integrate the whole process of the MOR, reduced model computation, and comparison and verification.

The paper is organized as follows: The governing thermal equation and its matrix format are first introduced in Section 2. Section 3 elucidates the algorithm of the trajectory piecewise linear model order reduction, which is followed by the MOR verification and demonstration using two relevant case studies (Section 4). The paper is finally summarized in Section 5.

GOVERNING EQUATION AND MATRIX FORMAT

The governing thermal equation for the spacecraft thermal analysis is given in Eq. (1). The discretization of the spatial differentials in the equation (or termed semi-discretization) leads to a nonlinear dynamic system (DAEs/ODEs) with temperature terms up to the 4th order (assuming constant thermal conductivity):

$$C_i \frac{dT_i}{dt} = \sum_{i \neq j} K_{ij}\left(T_j - T_i\right) + \sum_{i \neq j} R_{ij}\left(T_j^4 - T_i^4\right) - R_{si} T_i^4 + Q_i \tag{1}$$

where T_i, C_i, and Q_i are, respectively, the temperature, thermal capacitance, and heat source of the i^{th} node (i=1,2…n), and n is the total number of nodes. Note that Q_i includes internal heat generation (electronics heating) and environmental fluxes (e.g., solar radiation) at the boundary[1]; K_{ij} and R_{ij} are, respectively, the conductive and radiative conductors between nodes, and R_{si} is the radiative conductor between the i^{th} node and deep space. Eq. (1) can be cast into a compact matrix form as follows:

$$C \frac{dT}{dt} = f\left(T\right) + D \cdot u \quad \text{where} \quad f\left(T\right) = A \cdot T + B \cdot T^4 \tag{2}$$

where $T(t) \in \Re^{\mathrm{n}}$ is a vector denoting the temperature at all the nodes; t is time; $A \in \Re^{\mathrm{n \times n}}$ and $B \in \Re^{\mathrm{n \times n}}$ respectively derive from the conductive and radiative conductors in Eq. (1); $D \in \Re^{\mathrm{n \times m}}$ is the correlation matrix assigning internal heat source and environmental flux into each node; f describes the nonlinear contribution from conduction and radiation to the temporal differential of nodal temperatures. The model reduction is essentially to reduce the dimension of T in the original system to order $k \ll n$ through projection (i.e., $T = U_r T_r$) onto a low-dimensional space $U_r \in \Re^{n \times k}$ while retaining the same number of thermal inputs, i.e.,

$$C\frac{dT}{dt}=f\left(T\right)+D\cdot u \overset{T=U_rT_r}{\rightleftarrows} U_r^T C U_r \frac{dT_r}{dt}=U_r^T f\left(U_r T_r\right)+U_r^T D\cdot u \tag{3}$$

where $T_r(t)\in\Re^k$ is the temperature in the reduced system. Due to the greatly lower dimension of the reduced system relative to the original system (i.e., $k \ll n$) and the use of the ODE/DAE solvers that rely on the matrix manipulation simultaneously on all nodes (rather than node-wise), the computational cost drops down significantly. Accordingly, the most critical step for generating reduced thermal model is to construct the low-dimensional projection space U_r as shown in the next section.

TRAJECTORY PIECEWISE-LINEAR MODEL ORDER REDUCTION (TPWLMOR)

In this section, we present the algorithm formulation and implementation of the Trajectory Piecewise-Linear Model Order Reduction (TPWLMOR) for the spacecraft thermal analysis. In contrast to the other nonlinear MOR approach (in particular, the Proper Orthogonal Decomposition-POD)[2], TPWLMOR can generate reduced models without simulating the original full-scale model[3]. The TPWLMOR technique combines linear MOR algorithm and the concept of piecewise-linear (PWL) approximation. The MOR algorithm is used to find a series of linearization points along a typical trajectory, where local projection space U_p can be determined to reduce the full-scale models around the linearization points. The local projection space can then be gathered to construct a global projection space U_k. On the other hand, the PWL approximation builds a global reduced model based on the weighted combination of the linearized low-dimensional models at the linearization points (along the trajectory) to mimic the behavior of the original nonlinear system. The procedure can be divided into three key steps as outlined below:

Creating Reduced Model around the Linearization Points

The nonlinear function $f(T)$ above can be approximated using Taylor expansion about a certain temperature vector T_i, yielding

$$f\left(T\right)\approx f\left(T_p\right)+H_p\left(T-T_p\right) \tag{4}$$

where H_p is the Jacobian of $f(T)$ evaluated at T_p. Given s linearization points T_1, T_2, $T_p\ldots T_s$, we can obtain s linearized full models, which are given by

$$CdT/dt=H_pT+\left(f\left(T_p\right)-H_pT_p\right)+D\cdot u=H_pT+\bar{D}\cdot\bar{u} \quad \text{and} \quad p=1,2,\ldots s \tag{5}$$

where $\bar{D}=\left[f\left(T_p\right)-H_pT_p \quad D\right]$ and $\bar{u}=\left[1 \quad u\right]^T$, i.e., the term $f(T_p)$-H_pT_p is treated as a constant input in the linearized model.

A linear MOR method, such as a Krylov approach[3,4] and the Poor Man Truncated Balanced Realization (PMTBR)[5] is then used to identify a projection subspace $U_p\in\Re^{k\times n}$ and reduce the linearized full-scale model to dimension k at the linearization point T_p, yielding

$$C_p^k dT_k^p/dt=H_p^k T_k^p+\bar{D}_p^k\cdot\bar{u} \quad \text{and} \quad p=1,2,\ldots s \tag{6}$$

where $C_p^k=U_p^T C U_p$, $H_p^k=U_p^T H_p U_p$, $\bar{D}_p^k=U_p^T\bar{D}$, and $T_k^p$is the approximate solution of T_p on the p^{th} projection subspace, i.e., $Tp = U_pT_k^p$. Simulate the reduced linear model in Eq.(6) and determine the next linearization point T_{p+1}, while $U_pT_k^{p+1}$ is close enough to the initial linearization point T_p, i.e., $\|U_pT_k^{p+1}\text{-}T_p\|/\|T_p\|<\varepsilon$, where ε is an appropriately selected constant. This procedure is continued till the end of the trajectory.

Creating the Global Projection Subspace

Given the local projection subspace U_p from the last step, we can extract the global projection subspace U_r using single value decomposition (SVD). The global projection subspace U_r is then used to reduce the local linearized full-scale models.

Specifically, we define $P = [U_1, U_2,\ldots U_p,\ldots\ U_s]$, where P is the union of U_p.

Take a SVD of P to orthogonalize its column components, and construct the new global projection space U_r. by $P \approx U_r\Sigma_r V_r^{\mathrm{T}}$.

The p local linearized reduced models can then be obtained by

$$C_p^r dT_r \big/ dt = H_p^r T_r + \bar{D}_p^r \cdot \bar{u} \quad \text{and} \quad p = 1,2,\ldots s \tag{7}$$

where $C_p^r = U_r^T C U_r$, $H_p^r = U_r^T H_p U_r$, $\bar{D}_p^r = U_r^T \bar{D}$, and T_r is the approximate solution of T on the global projection space, i.e., $T = U_rT_r$.

Generation of TPWL Reduced Thermal Model

Next we construct the global TPWL reduced thermal models as a weighted combination of the local linearized reduced models (i.e., Eq. (7)), which is given by:

$$\left(\sum_{p=1}^{s} w_p(T_r) C_p^r\right) dT_r \Big/ dt = \left(\sum_{p=1}^{s} w_p(T_r) H_p^r\right) T_r + \left(\sum_{p=1}^{s} w_p(T_r)\, \bar{D}_p^r\right) \bar{u} \quad \text{and} \quad \sum_{p=1}^{s} w_p(T_r) = 1 \tag{8}$$

The temperature-dependent weight w_p represents the impacts of the p-th linearized reduced model to the global model. During a transient analysis, w_p at each time step is determined by the following procedure: 1) for p = 1,…s, compute $d_p = \|T\text{-}T_p\|_2 = \|T_r\text{-}U_r^{\mathrm{T}}T_p\|_2$; 2) take m = min (d_p) for p = 1,…s; 3) for p = 1,…s, compute ω_p = $e^{-\lambda dp/m}$; and 4) normalize ω_p. Set $w_p(T_r) = \omega_p(T_r) \Big/ \sum_{p=0}^{s-1} \omega_p(T_r)$. Figure 1 summarizes the TPWLMOR algorithm. The TPWLMOR algorithm formulated in this paper was implemented in Matlab.

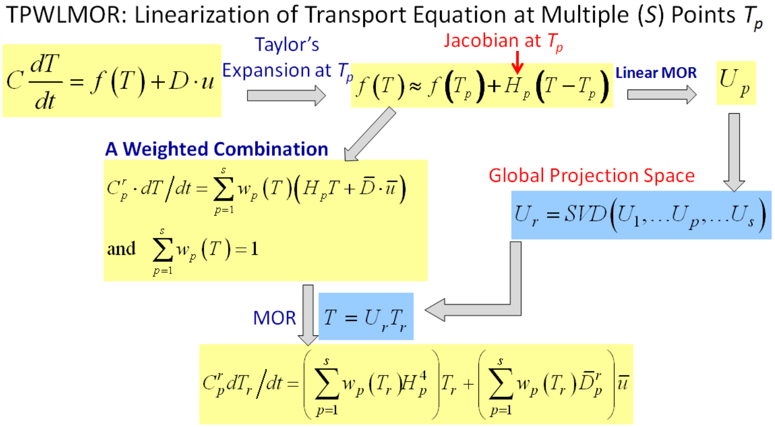
TPWLMOR: Linearization of Transport Equation at Multiple (S) Points T_p
$C\frac{dT}{dt} = f(T) + D\cdot u$
Taylor's Expansion at T_p
Jacobian at T_p
$f(T) \approx f(T_p) + H_p(T - T_p)$
Linear MOR
U_p
A Weighted Combination
$C_p^r \cdot dT/dt = \sum_{p=1}^{s} w_p(T)(H_pT + \bar{D}\cdot\bar{u})$
and $\sum_{p=1}^{s} w_p(T) = 1$
Global Projection Space
$U_r = SVD(U_1,\ldots U_p,\ldots U_s)$
MOR
$T = U_rT_r$
$C_p^r dT_r/dt = \left(\sum_{p=1}^{s} w_p(T_r)H_p^4\right)T_r + \left(\sum_{p=1}^{s} w_p(T_r)\bar{D}_p^r\right)\bar{u}$

Figure 1. Flow chart for constructing the reduced order models with TPWLMOR

RESULTS AND DISCUSSION

In this section, we demonstrate the application of our MOR simulation tool to NASA-relevant case studies of thermal analysis, and compare the results against SINDA/FLUINT (S/F) for technology validation. Two key steps are involved in converting the full-scale S/F models to the reduced order models (ROM): (1) data export & model assembly and (2) MOR. The former extracts the model descriptive information from S/F and assemble the full-scale models amenable to Matlab simulation (referenced as Matlab full-scale model below); and the latter yields the ROM from the full-scale Matlab model for reduced order analysis. Therefore, both of them were verified by comparing ROM, full-scale Matlab, and S/F data in terms of steady-state and transient temperature distribution. The steady-state results in our ROM were obtained by simulating the transient thermal equilibrating process assuming an arbitrarily initial temperature (e.g., 0°C). Two testbed thermal models[6] of LISA with different computational sizes were investigated (see Table 1). LISA is a constellation mission designed to detect and observe gravitational waves in the 0.1 mHz to 0.1 Hz frequency band. The small LISA model contains 618 nodes while the mid-size LISA 2874 nodes. In the transient analysis of both models, the solar frequencies are, respectively, set at 0.1 and 1 mHZ with 1% fluctuation in solar intensity (around the steady-state values.) The full-scale Matlab model and ROMs were simulated in the script mode on a multi-user server equipped with a 3 GHz AMD Athlon 64 X2 Dual Core Processor 6000+ and 4 GB RAM.

To quantitatively characterize the discrepancy between the full-scale model and ROM, two performance indices were defined in the verification module of our simulation tool: the absolute error and the rms error, which are given by

$$Err_{abs} = U_r T_r^{abs} - T_{full}^{abs} \tag{9}$$

$$Err_{rms} = \sqrt{\sum_{i=1}^{N_s} \left(U_r T_r^{abs} - T_{full}^{abs} \right)^2 \Big/ \sum_{i=1}^{N_s} \left(T_{full}^{abs} \right)^2} \tag{10}$$

where T_r^{abs} and T_{full}^{abs} are the absolute temperature data from ROM and full-scale models; and N_s is the number of nodes in the model over which the rms error is evaluated. Note that Err_{abs} is a vector and represents the temperature difference between the full-scale model and ROM for each node, while Err_{rms} is the average relative error in the entire computational domain. In addition, by removing the summation symbol in Eq. (10) we can assess the node-wise relative error, which was used in the steady-state simulation below.

Table 1. LISA models for Phase I MOR case studies

	Computational Orders	Initial Temperature for Steady-State Simulation (C)	Solar Frequency (mHz)	Solar Fluctuation
Small LISA	618	0	0.1, 1	0.01
Mid-Size LISA	2874	0 and 20	0.1, 1	0.01

Small-size LISA Thermal Model

Figure 2 illustrates the comparison between TPWLMOR, full-scale Matlab and S/F for the small-size LISA model on the steady-state solution. The temperature spans a wide range from –122 °C to 86 °C (Figure 2a). Figure 2b depicts the equilibrating process starting from the initial temperature at 0 °C. The full-scale Matlab model shows excellent agreement with the S/F data with the largest relative error of 0.042%, which convincingly verifies our data export and model assembly procedure. The comparison between TPWLMOR, full-scale Matlab model and S/F data in terms of both steady-state (Figure 2a) and equilibrating-process solution (Figure 2b) exhibits excellent agreement with the absolute node-wise temperature errors ranging from -1 to +0.5 °C (mostly restricted between -0.3 and +0.3°C) yielding an average relative error less than 0.1%.

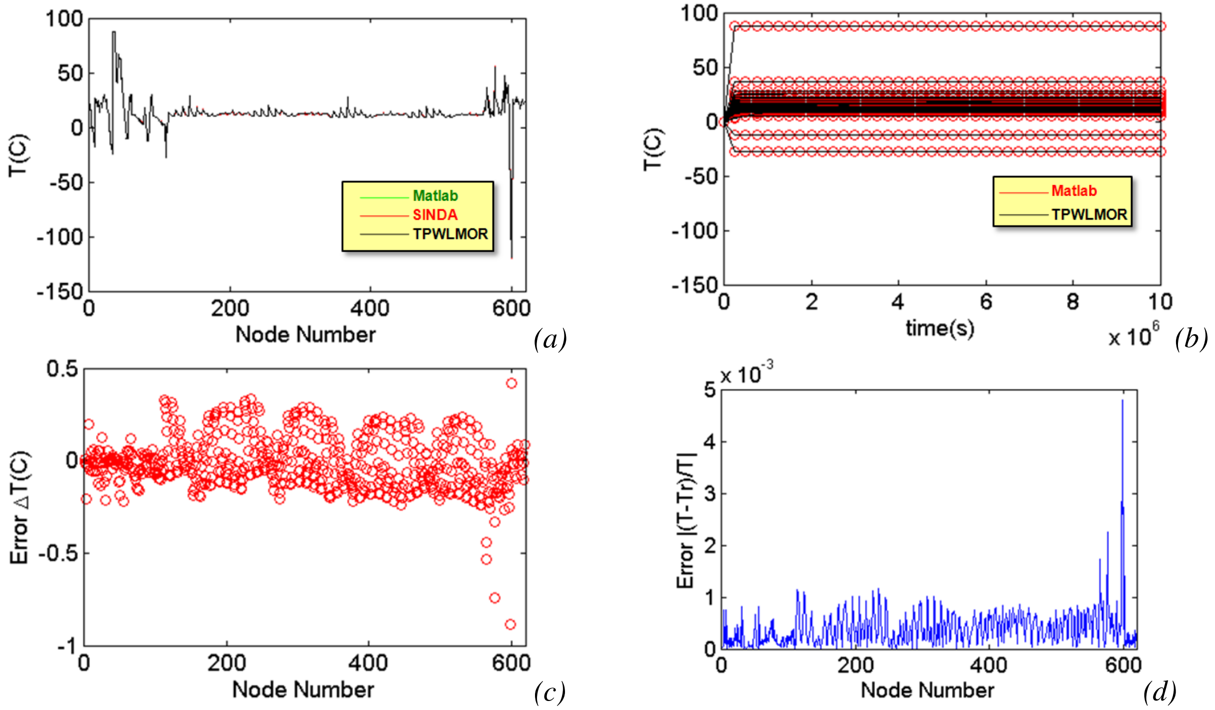

Figure 2. Comparison between TPWLMOR, full Matlab model, and S/F for steady-state temperature distribution in the small-size LISA model (a) node-wise temperature, (b) the equilibration process (51 nodes selected at an interval of 12 nodes), (c) absolute error in node-wise temperature, and (d) relative error.

Figure 3 illustrate the comparison between TPWLMOR, full-scale Matlab, and S/F data in terms of transient temperature distribution with the solar fluctuation frequency of 1 mHz. The ROM generated from the simulation of the equilibrating process was reused here. The steady-state solution obtained above was used as the initial condition for the transient analysis. TPWLMOR results show excellent agreement with full-scale Matlab and S/F data in the temporal domain at all times (Figure 3a). For graphical clarity, 51 nodes are selected from the 618 nodes in the small-size LISA at an interval of 12 nodes. Strongest temperature oscillation (Figure 3b) due to the external solar fluctuation is clearly observed at the node carrying the highest temperature, which however smears out within the satellite and becomes negligible at the node with the lowest temperature. Figure 3c depicts the absolute errors in the node-wise temperature and their temporal dependence, which are similar to the steady-state simulation. The worst relative error of the entire computational domain as shown in Figure 3d is 0.5% with most of them falling far below 0.1% signifying excellent overall match between TPWLMOR and S/F data. The simulation results for the solar frequency of 0.1 mHz are similar and are not shown here.

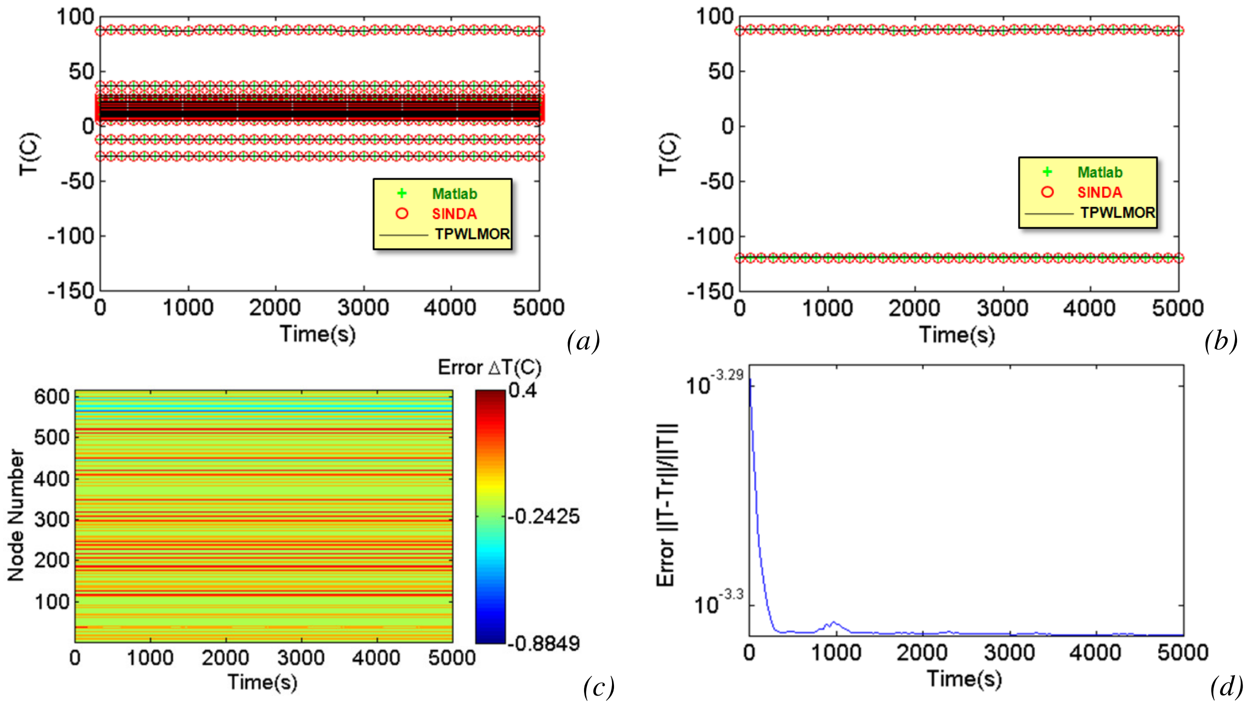

Figure 3. Comparison between TPWLMOR, full-scale Matlab model, and S/F data for transient temperature distribution with a solar fluctuation frequency of 1 mHz for the small LISA model (a) transient node-wise temperature, (b) nodes with highest and lowest temperature, (c) absolute error in node-wise temperature, (d) average relative error.

Mid-size LISA Thermal Model

Figure 4a and Figure 4b show the comparison between TPWLMOR, full-scale Matlab, and S/F data in terms of the steady-state temperature profile and equilibrating process in the mid-size LISA model. The full-scale Matlab model matches the S/F model very well with the maximum node-wise relative error of 0.17%, which again verifies the data exchange interface and model assembly procedure. Good agreement is observed between TPWLMOR and S/F data with the absolute temperature error spanning from -2.8°C to +2.9 °C (Figure 4c). The worst node-wise relative error is ~2% with most of them <0.5%.

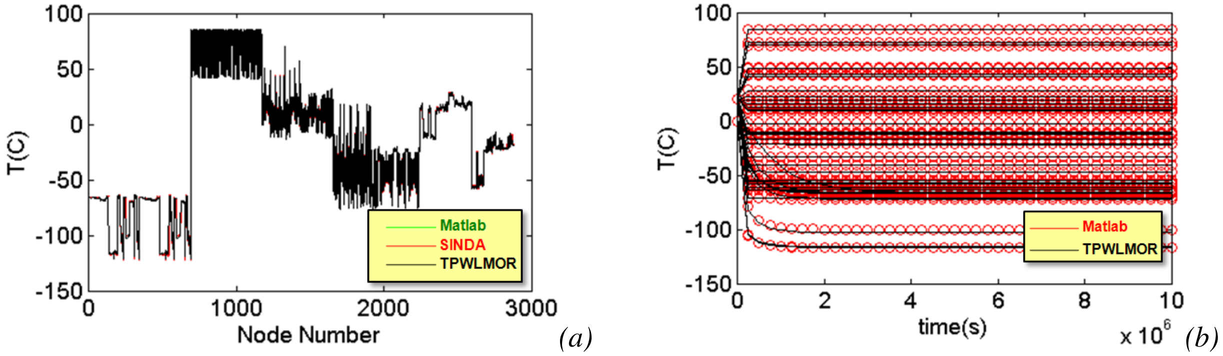

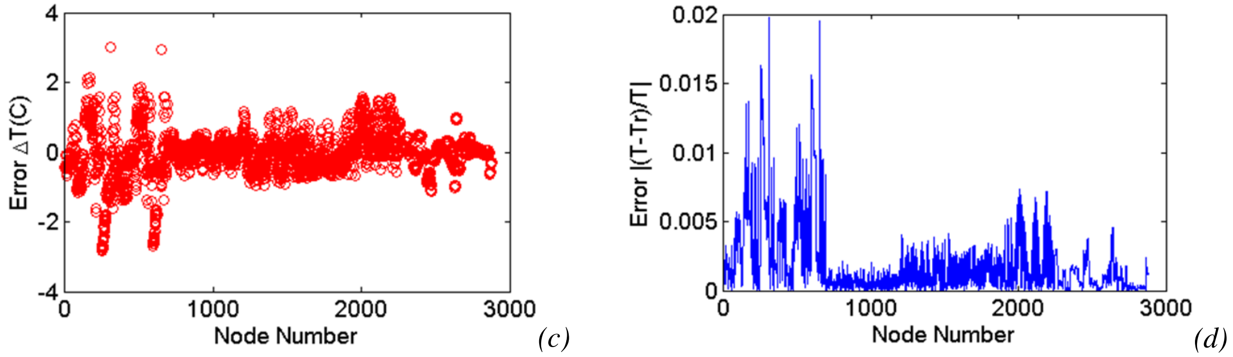

Figure 4. Comparison between TPWLMOR, full Matlab model, and SINDA/FLUINT for steady-state temperature distribution in the mid-size LISA model (a) node-wise temperature, (b) the equilibration process (47 nodes selected at an interval of 60 nodes), (c) absolute error in node-wise temperature, (d) relative error.

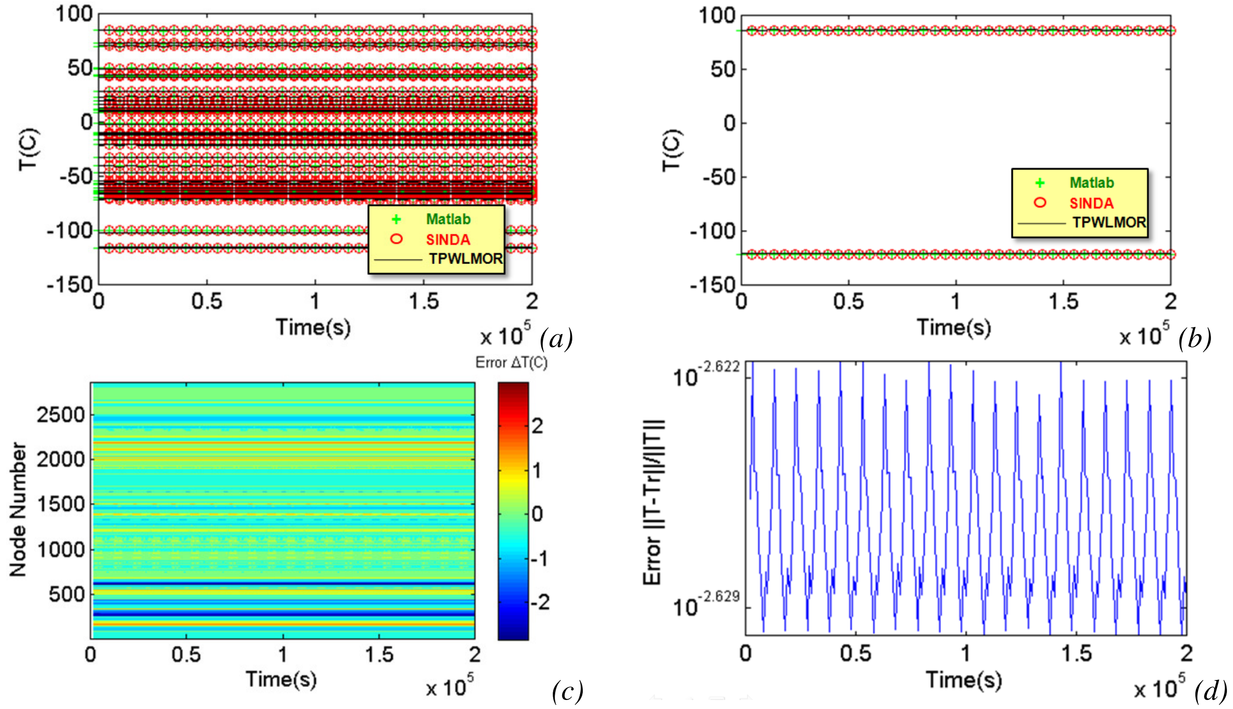

Figure 5. Comparison between TPWLMOR, full Matlab model, and SINDA/FLUINT for transient temperature distribution with a solar fluctuation frequency of 0.1 mHz for mid-size LISA model (a) transient node-wise temperature (b) nodes with highest and lowest temperature, (c) absolute error in node-wise temperature, (d) relative error.

Figure 5 illustrate the comparison between TPWLMOR, full-scale Matlab model, and S/F data on the transient temperature profile using solar fluctuation frequency of 0.1 mHz. The steady-state solution from the previous simulation (Figure 4) was used as the initial condition. TPWLMOR exhibits excellent accords with the full-scale S/F model at all times. Temperature oscillation (Figure 5b) of the solar array carrying the highest temperature evaluated by all models is slightly flatter than that in the small-size LISA model. The absolute error in the node-wise temperature and its temporal dependence are plotted in Figure 5c, and within (-2.8°C, +2.9 °C).

The average relative error of all nodes in the entire domain is <0.5% indicating notable overall performance of TPWLMOR (Figure 5d). Likewise, the transient simulation results with the solar frequency of 1 mHz are similar and not shown here.

ROM Performance

The computational performance of ROM, full-scale Matlab and S/F model are compared in Table 2 and Table 3, respectively, for the small-size and mid-size LISA models. For the small-size model, it took 16.2 and 1.08 s, respectively, for ROM generation (with 64 orders) and computation in the steady-state analysis. The full-scale Matlab was completed in 10.7 s. It should be pointed out that the model generation is a one-time cost and the generated ROM can be reused for various operating scenarios. For example, the ROM obtained from the steady-state simulation was also used in the transient simulation involving fluctuating solar flux at different oscillating frequencies (0.1 and 1 mHz) as shown in Table 2. Discounting the model generation time, our ROM enables a salient speedup over the full-scale Matlab model without appreciable compromise in simulation accuracy. Note that as both ROM and full-scale Matlab model rely on the sparse matrix operation simultaneously on all nodes during ROM integration, additional acceleration can be obtained if a node-wise iterative solution process is used as the benchmark for comparison (this will be the typical case for larger thermal models). As the S/F model uses a computational platform and convergence criterion (1×10^{-12} °C) distinctly different from our ROM integration (relative tolerance 1×10^{-4}) a direct comparison between ROM and S/F on the computational time is not made in this case.

The comparison of the computational performance for the mid-size LISA model is summarized in Table 3. In the steady-state simulation, it took 341.8 s and 1.6 s, respectively, for ROM generation (with 64 orders) and integration, while the full-scale Matlab analysis entailed 260 s. For the transient simulation, the full-scale Matlab model and S/F were completed within ~300 s and ~600 s as opposed to 1 s using ROM. **This yields a 150–900X acceleration in the computational speed** along with order-of-magnitude savings in physical memory due to the significantly reduced model orders. As discussed previously, the model generation time depends on the accuracy requirement and the number of reduced orders. Relaxation in accuracy can further lower the computational cost of ROM, and justify the practical values of ROM for spacecraft thermal analysis.

Table 2. Comparison between TPWLMOR, full-scale Matlab, and SINDA/FLUINT simulation for small-size LISA model

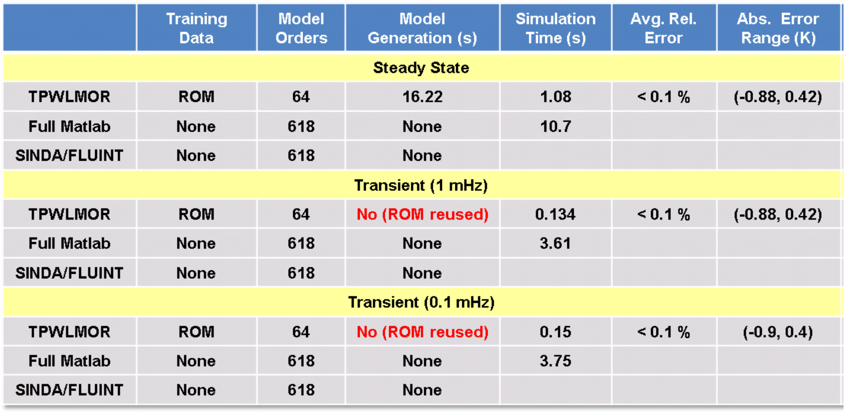

	Training Data	Model Orders	Model Generation (s)	Simulation Time (s)	Avg. Rel. Error	Abs. Error Range (K)
			Steady State			
TPWLMOR	ROM	64	16.22	1.08	< 0.1 %	(-0.88, 0.42)
Full Matlab	None	618	None	10.7		
SINDA/FLUINT	None	618	None			
			Transient (1 mHz)			
TPWLMOR	ROM	64	No (ROM reused)	0.134	< 0.1 %	(-0.88, 0.42)
Full Matlab	None	618	None	3.61		
SINDA/FLUINT	None	618	None			
			Transient (0.1 mHz)			
TPWLMOR	ROM	64	No (ROM reused)	0.15	< 0.1 %	(-0.9, 0.4)
Full Matlab	None	618	None	3.75		
SINDA/FLUINT	None	618	None			

Table 3. Comparison between TPWLMOR, full-scale Matlab, and SINDA/FLUINT simulation for mid-size LISA model

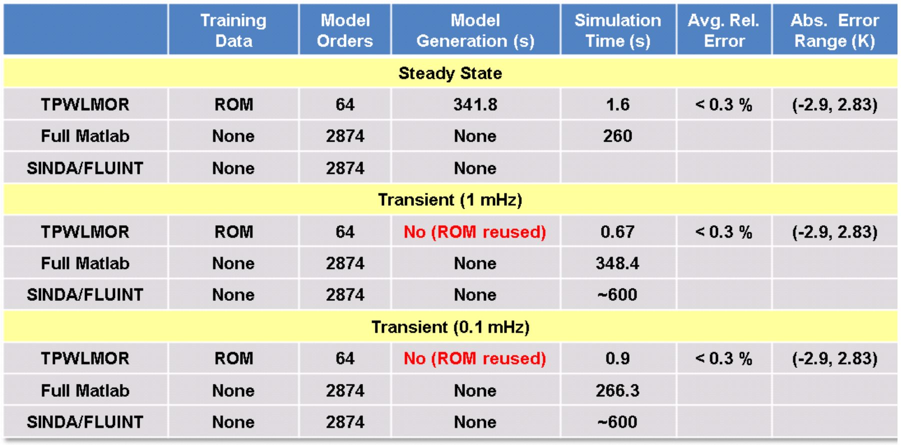

	Training Data	Model Orders	Model Generation (s)	Simulation Time (s)	Avg. Rel. Error	Abs. Error Range (K)
Steady State						
TPWLMOR	ROM	64	341.8	1.6	< 0.3 %	(-2.9, 2.83)
Full Matlab	None	2874	None	260		
SINDA/FLUINT	None	2874	None			
Transient (1 mHz)						
TPWLMOR	ROM	64	No (ROM reused)	0.67	< 0.3 %	(-2.9, 2.83)
Full Matlab	None	2874	None	348.4		
SINDA/FLUINT	None	2874	None	~600		
Transient (0.1 mHz)						
TPWLMOR	ROM	64	No (ROM reused)	0.9	< 0.3 %	(-2.9, 2.83)
Full Matlab	None	2874	None	266.3		
SINDA/FLUINT	None	2874	None	~600		

CONCLUSIONS

In this paper, we presented a novel projection-based Model Order Reduction (MOR) simulation tool for fast and efficient spacecraft thermal analysis. The tool provides a holistic simulation capability by integrating the data export & model assembly, MOR engine, DAE integration solver, comparison and verification module on a unified, modular framework. The MOR engine is based on the mathematically rigorous Trajectory Piece-Wise Linear MOR (TPWLMOR) algorithm to enable automated generation of reduced thermal models. Due to the low-dimensional nature of the reduced thermal models, the DAE integration solver relying on the matrix manipulation can be exploited for fast analysis.

The simulation results of two testbed models containing roughly ~600 and ~3000 nodes and consisting of constant sources, capacitances, and conductances were used to evaluate the TPWLMOR engine and solver. The full-scale models were reduced to low-dimensional models with 64 nodes. The overall MATLAB solution of the reduced model took about 1 second compared to ~10 and ~300 seconds for the full-scale solution. Excellent agreement between the reduced and full-scale solution with the maximum absolute nodal temperature error spanning from -2.8°C to +2.9 °C (primarily between -1 °C and +1 °C) and the average relative error of less than 0.5% were achieved. The computational expense incurred to generate the reduced model is a one-time cost and becomes less important as the model sizes increase. The reusability of ROM enables significant savings in computational times and resources for transient simulation and analysis. The case studies successfully establish the feasibility of our MOR technique for spacecraft thermal analysis.

The future work will be focused on the development of new model/simulation capabilities (e.g., temperature-dependent conductors, time-dependent boundary conditions, and parameterized MOR), the algorithm refinement for enhanced accuracy, and software optimization for improved execution efficiency. In addition, we will also explore the potential of propagating our MOR technology to other NASA-relevant research arenas, such as fluidic and active thermal, aerothermal, and structural analysis.

ACKNOWLEDGEMENTS

This research is sponsored by NASA under contract number NNX11CB02C.

CONTACT

Corresponding author: Yi Wang
CFD Research Corporation, 215 Wynn Drive, Suite 501, Huntsville, AL 35805
Phone: (256) 327-0678; Fax: (256) 327-0985; Email: yxw@cfdrc.com
Web: http://www.cfdrc.com

NOMENCLATURE, ACRONYMS, ABBREVIATIONS

Symbols:

A	Matrix collecting conductive conductors
B	Matrix collecting radiative conductors
C	Thermal capacitance
D	Correlation matrix
d	Distance between the temperature vector and the linearization point
T	Temperature
H	Jacobian of nonlinear function $f(T)$
K	Conductive conductor
k	The order of the reduced thermal model
P	Union of the local projection space
Q	Heat flux
R	Radiative conductor
R_{si}	Radiative conductor to space
s	Number of the linearization points along the typical trajectory
t	The time
U	The left singular matrix or projection space
u	The thermal inputs
V	The right singular matrix
ω	Weights for each linearized reduced order model
w	Normalized weights for each linearized reduced order model

Subscripts/Superscripts:

$full$	Full model results
i	The i^{th} node
j	The j^{th} node
ij	Between the i^{th} and j^{th} node
r	The reduced order models in the global projection subspace
p	The p^{th} linearization points along the typical trajectory
k	The reduced order models in the local projection subspace

REFERENCES

(1) Tsai, J. R. *Journal of Spacecraft and Rockets* **2004**, *41*, 120-125.

(2) Aling, H.; Kosut, R. L.; Emami-Naeini, A.; Ebert, J. L., Kobe, Japan, December 1996; 4305-4310.

(3) Yang, Y. J.; Shen, K. Y. *Journal of Micromechanics and Microengineering* **2005**, *15*, 408-418.

(4) Odabasioglu, A.; Celik, M.; Pileggi, L. T. *IEEE Transactions on Computer-Aided Design of Integrated Circuits and Systems* **1998**, *17*, 645-654.

(5) Phillips, J. R.; Silveira, L. M. *Ieee Transactions on Computer-Aided Design of Integrated Circuits and Systems* **2005**, *24*, 43-55.

(6) Peabody, H.; Merkowitz, S. 2005; Iop Publishing Ltd; S403-S411.